Turkish Journal of Chemistry
http://journals.tubitak.gov.tr/chem/
Research Article

Turk J Chem
(2019) 43: 73 – 83
© TÜBİTAK
doi:10.3906/kim-1806-27

Electrodeposition of tin(II) from citrate complexes

Yuliya YAPONTSEVA, Valeriy KUBLANOVSKY*
V. I. Vernadskii Institute of General and Inorganic Chemistry of the National Academy of Sciences of Ukraine, Kyiv, Ukraine

Received: 09.06.2018 • **Accepted/Published Online:** 08.10.2018 • **Final Version:** 05.02.2019

Abstract: This paper provides the calculation of the distribution of the concentrations of complex particles of the Sn(II) - citrate - water system in the solution volume, on the surface of the electrode, and in the diffusion layer for the tin citrate electrolyte containing an excess of the ligand. Based on the calculations for the electrodeposition of tin, an electrolyte containing $[SnCit]^{2-}$ complex at pH 8.0 was chosen. The kinetic parameters of the discharge stage, the diffusion coefficient of the electrochemical active ion, and the current efficiency of tin were determined by the methods of stationary voltammetry and chronovoltamperometry. It is shown that the electroreduction of tin is governed by the laws of mixed kinetics and the transfer stage of the second electron is the limiting one. The discharge mechanism and the composition of the electroactive complex, which is $[SnCit]^{2-}$, are proposed. The current density of the deposition of tin coatings with different functional properties is determined as protective coatings and coatings of anodes of Li-ion accumulators.

Key words: Tin, citrate complex, electroreduction

1. Introduction

In modern science and technology, great efforts are made to develop high-density compact power sources for portable electronics and electronic vehicles. The most promising of them are lithium-ion batteries, the efficiency of which depends, among other factors, on the capacity of the anodic materials used.[1] Some of the possible candidates for the replacement of the existing graphite anodes are tin, thanks to its high theoretical specific capacity (994 mAh g^{-1}), and tin-rich alloys, such as Sn-Ni, Sn-Cu, and Sn-Co. In theory, the capacity of a tin anode is three times higher than that of commercial graphite anodes; however, tin loses most of its capacity during cycling because of an increase in volume during lithium intercalation and coating structure disturbance, i.e. surface failure and sputtering of the active substance.[2] In a previous work,[3] the electrodeposition and properties of films deposited from tartrate, citrate, and citrate-trilonate electrolytes were investigated; it was shown that the films electrodeposited from a citrate electrolyte had the best charge-discharge characteristics in lithium power sources. The efficiency of citrate solutions was also shown during the electrodeposition of Sn-Cu alloys, which have high corrosion resistance.[4]

The study of the electroreduction of Sn^{2+} citrate complexes in acid media is dealt with in a number of papers.[5–8] One such study reported a calculation of electrolyte components under equilibrium conditions and on the electrode surface.[7] The main object of investigation there was an acid electrolyte containing protonated tin(II) and cobalt(II) complexes. The kinetics of $[SnHCit]^-$ reduction in an electrolyte containing no free citrate

*Correspondence: kublanovsky@ionc.kar.net

have been studied. It has been concluded that a low pH value and the absence of free ligand are necessary conditions for the convergence of the potentials for the separation of Sn and Co, and for the deposition of high-quality Sn-Co alloys from citrate electrolytes. The paper did not present a calculation of the distribution of ligand species in the bulk electrolyte as a function of pH, which is necessary for the correct description of the tin citrate electroreduction mechanism and for the explanation of the causes of adsorption and desorption of species of a definite composition.

Another work presented distribution diagrams of ionic species of tin citrate and ligand as a function of pH at different ligand excesses.[8] The calculation involves no instability constant and hence no material balance equation for the unprotonated ligand species and unprotonated tin citrate complex. In view of this, the existence at neutral pH of two protonated ligand species and a protonated tin citrate species in the solution under equilibrium conditions, and all the more so during electrolysis with alkalization of the near-electrode layer, seems to be very doubtful.

Electrodeposition of metals from complex electrolytes is a complicated multistage process. The concentration of complex particles of each species in the volume of the solution depends not only on the pH, but also on the metal-ligand ratio. The presence of a free ligand ensures the complete binding of metal ions and thus eliminates the parallel discharge on the cathode of solvated metal ions, which passes with much less overvoltage than the discharge of a complex ion. A large overvoltage of the cathode reaction ensures the formation of finer crystalline precipitates, and the predictability of the composition of the reacting particles makes it possible to accurately control the coating quality and the stability of the electrolyte operation. Comparison of works known from the literature does not give an accurate picture of the distribution of citrate complexes of tin and citrate over a wide pH range and in the presence of an excess of ligand.

Thus, the concepts of the kinetics and discharge mechanism of Sn citrate complexes in neutral and slightly alkaline media are debatable. Therefore, the aim of this work is to determine the laws governing the discharge of $[SnCit]^{2-}$ complexes by modeling the volumetric and surface composition of a citrate electrolyte for Sn deposition in conjunction with experimental data.

2. Results and discussion

2.1. State of ions in the bulk solution

To investigate the processes of deposition of metals from solutions of their complex compounds, information on the distribution of different complexes and ligand species in the bulk solution is required in the first place.[9]

To determine the composition of ions in the bulk electrolyte, a closed system of equations was set up, which reflects the laws of material balance, electroneutrality, and mass action:

$$Sn^{2+} + pCit^{4-} + qH^{+} \Leftrightarrow SnCit_pH_q^{2+q-4p}, \tag{1}$$

where p and q are stoichiometric coefficients.

$$C_{Sn^{2+}} = \left[Sn^{2+}\right] + \sum_{i=0}^{i=1} [SnCitH_i]; \tag{2}$$

$$C_{Cit} = \sum_{i=1}^{i=3} [SnCitH_i] + 2 \cdot \left[SnCit_2\,(OH)_2^{8-}\right] + \sum_{i=0}^{i=4} [H_iCit]. \tag{3}$$

The law of electroneutrality:

$$\sum zc = 0; \tag{4}$$

and equations for complex ion formation constants:

$$\beta_{[SnCit^{2-}]} = \frac{[Cit^{4-}] \cdot [Sn^{2+}]}{[SnCit^{2-}]}, \tag{5}$$

$$\beta_{[SnCitH^{-}]} = \frac{[Cit^{4-}] \cdot [Sn^{2+}] \cdot [H^{+}]}{[SnCitH^{-}]}. \tag{6}$$

Formation constant values of corresponding tin complexes are $\lg\beta_{\ [SnCitH]} = 19.5$ and $\lg\beta_{\ [SnCit]} = 15.35$.[10]

The distribution of tin and citrate complex species as a function of pH is shown graphically in Figure 1.

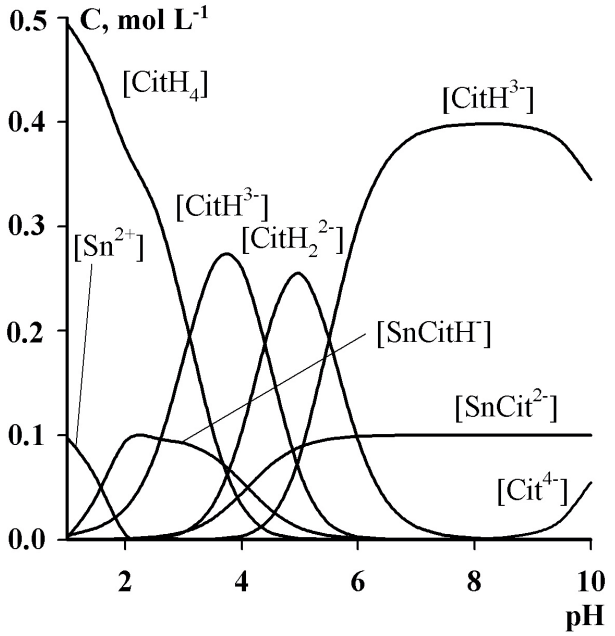

Figure 1. Distribution of ionic species in the bulk solution as a function of pH for tin(II) complexes at the ratio of $[Sn^{2+}] : [Cit^{4-}] = 1 : 5$.

As seen from Figure 1, solvated tin(II) ions exist in the electrolyte only in the very acidic region in the pH range of 0–2. The protonated tin citrate complex is in the bulk solution in the pH range of 1–5, and in the acidic pH region it coexists with three protonated ligand species at the same time, the presence of which greatly complicates the research and the interpretation of the obtained data. Besides, at pH 0–5, undissociated citric acid is present in the solution. At pH 3, a normal tin citrate complex $[SnCit^{2-}]$ is already formed, and all tin exists in the solution as this complex. In the widest pH range, the existence of a protonated ligand is discernible, a free unprotonated ligand being formed even in an alkaline medium and only at pH of >9.

As will be mentioned below, the protonated ligand species can also be electrochemically reduced at the cathode, thereby increasing the current efficiency of hydrogen. The lower the pH value and the higher the protonation degree of the ligand, the higher the rate of the secondary process of hydrogen electroreduction.

Based on the above, a solution containing tin as the normal complex [$SnCit^{2-}$] and having a pH of 8.0 was chosen for the study of the electroreduction of tin citrate. The electrolyte contains a protonated ligand species [$CitH^{3-}$] and a small amount of [$CitH_2^{2-}$] and [Cit^{4-}].

2.2. Mass transfer in the diffusion layer

When studying the electroreduction kinetic of metals, information on the concentration distribution of the electrolyte components on the electrode surface and in the diffusion layer is required. Chemical interaction between the solution complex nature of concentration profiles in the diffusion layer was measured. The consequence of this are great differences in component distribution in the bulk solution and near the electrode surface.

In the case of current flow under the conditions of the stationary state of the system and the absence of specific adsorption, as well as slow chemical stages, the equation of total charge transfer for metal perpendicular to the electrode surface is of the form:

$$\frac{j_{Sn}}{2F} = D_{Sn^{2+}}\frac{\partial[Sn^{2+}]}{\partial x} + D_{SnCit^{2-}}\frac{\partial[SnCit^{2-}]}{\partial x} + \frac{F}{RT}\frac{\partial E}{\partial x}\left(2D_{Sn^{2+}}[Sn^{2+}] - 2D_{SnCit^{2-}}[SnCit^{2-}]\right), \quad (7)$$

and the charge transfer for hydrogen:

$$\begin{aligned}\frac{j_H}{F} &= D_{H^+}\frac{\partial[H^+]}{\partial x} - D_{OH^-}\frac{\partial[OH^-]}{\partial x} + D_{HCit^{3-}}\frac{\partial[HCit^{3-}]}{\partial x} \\ &+ \frac{F}{RT}\frac{\partial E}{\partial x}\left(D_{H^+}[H^+] - D_{OH^-}[OH^-] - 3D_{HCit^{3-}}[HCit^{3-}]\right)\end{aligned}. \quad (8)$$

For the ligand and supporting electrolyte ions (0.5 mol L^{-1} Na_2SO_4) that do not cross the electrode/electrolyte interface, the mass transport phenomena caused by the diffusion and migration of ions in an electric field must compensate one another, i.e. the diffusion and migration fluxes are equal and opposite in sign:

$$\begin{aligned}&D_{HCit^{3-}}\frac{\partial[HCit^{3-}]}{\partial x} + D_{Cit^{4-}}\frac{\partial[Cit^{4-}]}{\partial x} + D_{SnCit^{2-}}\frac{\partial[SnCit^{2-}]}{\partial x} + \\ &+\frac{F}{RT}\frac{\partial E}{\partial x}(-3D_{HCit^{3-}}[HCit^{3-}] - 4D_{Cit^{4-}}[Cit^{4-}] - 2D_{SnCit^{2-}}[SnCit^{2-}]) = 0\end{aligned}, \quad (9)$$

$$\frac{\partial[Na^+]}{\partial x} + \frac{F}{RT}\frac{\partial E}{\partial x}[Na^+] = 0, \quad (10)$$

$$\frac{\partial[SO_4^{2-}]}{\partial x} - 2\frac{F}{RT}\frac{\partial E}{\partial x}[SO_4^{2-}] = 0. \quad (11)$$

In these equations, D is the diffusion coefficient of the ith component, E(x) is electric potential, x is the distance from the electrode surface, and j_{Sn} and j_H are the electroreduction currents of tin and hydrogen ions, respectively. The remaining symbols are generally accepted.

Eqs. (7)–(11), supplemented with appropriate equilibrium constant equations for electroneutrality condition in the bulk solution,

$$\sum z_i c_i = 0, \quad (12)$$

and the ionic product of water,

$$[H^+][OH^-] = K_w, \quad (13)$$

describe the concentration variation of all ionic species that are present in the alkaline citrate electrolyte for tin plating. This system of equations has been numerically integrated by the Runge–Kutta method at the following boundary conditions:

$$[c_i]_{x=\delta} = [c_i]_0, \tag{14}$$

$$[c_i]_{x=0} = [c_i]_s, \tag{15}$$

where $[c_i]_0$ and $[c_i]_s$ are the concentrations of the ith component in the bulk electrolyte and on the electrode surface, respectively.

The initial data for calculation at 25 °C are as follows: $D_H^+ = 9.34 \times 10^{-9}$ M^2 s^{-1}; $D_{OH}^- = 5.28 \times 10^{-9}$ M^2 s^{-1}; [11] $D_i = 4 \times 10^{-10}$ M^2 s^{-1}; [12] $K_W = 1.00 \times 10^{-14}$; $\delta = 2.57 \times 10^{-5}$ m; $c_{Sn}^{2+} = 0.1$ mol L^{-1}; $c_{H4Cit} = 0.5$ mol L^{-1} and $c_{Na2SO4} = 0.5$ mol L^{-1}; $0 \leq j_{Sn} \leq 4$ mA cm^{-2}. Here, D_i is the diffusion coefficient of the tin citrate complexes (it was assumed that the diffusion coefficient of citric acid and its complexes must not differ greatly).

In the integration it was taken into account that the diffusion layer thickness under natural convection depends on current density: [13]

$$\delta = \delta_0 j^{-0.2}. \tag{16}$$

The diffusion layer thickness was determined experimentally from the dependence of the limiting diffusion current j_d on the bulk concentration of ions being reduced: [14]

$$\delta_0 = nFD_i c_{Sn^{2+}}/j_d. \tag{17}$$

The results of theoretical calculations are presented in Figure 2.

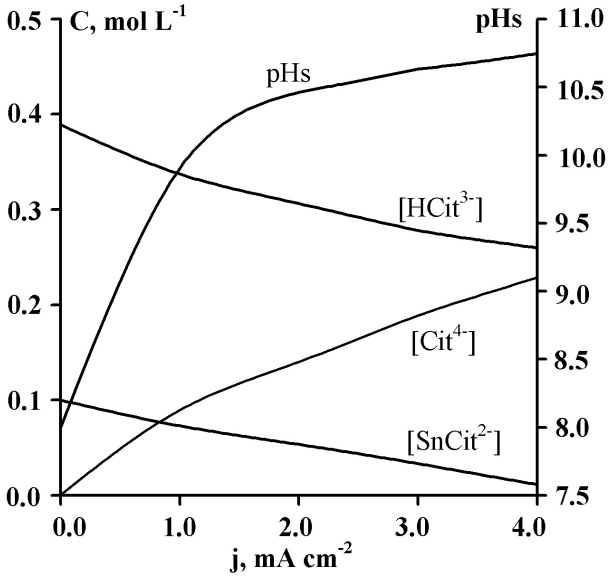

Figure 2. Dependence of the component concentration of a citrate electrolyte for tin plating on the cathode surface and surface pH on polarizing current density.

The surface concentration of tin citrate decreases at a constant rate with increasing current density and almost reaches zero at 4 mA cm^{-2}; at this current density value the experimental voltammetric curve exhibits

a limiting current plateau (Figure 2). The concentration of protonated ligand on the surface also decreases owing to the electroreduction of these species with hydrogen evolution on the same level as water molecules. Based on the shape of the curve and the rate of decrease in $[HCit^{3-}]$ surface concentration, it can be concluded that at high current densities, the concentration of protonated species decreases more slowly than in the current density range of 0–1 mA cm^{-2}, so the discharge of water molecules makes a greater contribution to the hydrogen evolution process. Because of the electroreduction of citrate complexes, the surface concentration of the free ligand constantly increases with current density. The electroreduction of protonated ligand species and water result in the fact that cathode surface pH_s increases in the course of electrolysis. The dependence of pH_s on polarizing current density is shown in Figure 2. At current densities close to the density limit, a strong alkalization of the cathode layer in comparison with the bulk electrolyte is observed for natural convection conditions, but the rate of pH_s change is already low.

To analyze the kinetics and mechanism of electroreduction of complexes, one must know not only surface concentrations, but also the concentration distribution of the components over the diffusion layer thickness. The result of this calculation is shown in Figures 3a and 3b. Under natural convection conditions, the concentration of all electrolyte components varies linearly from the value in the bulk solution to the value on the surface in Figure 3a.

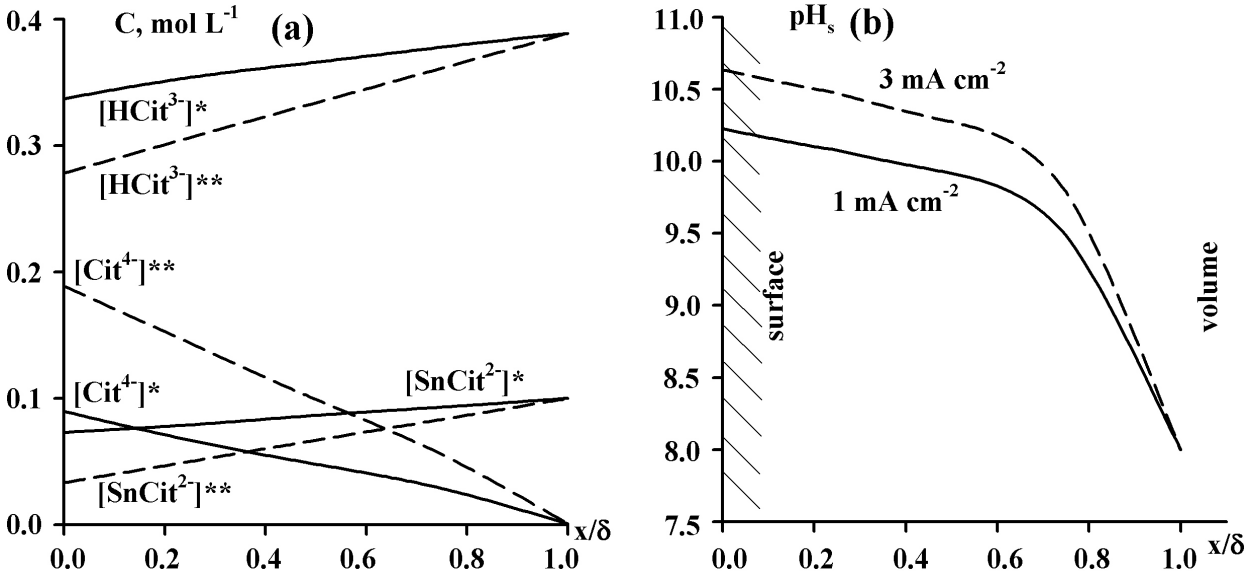

Figure 3. (a) Distribution of the concentration of the components of a citrate electrolyte for tin plating and pH over the diffusion layer thickness during electrolysis, (b) at two current densities: *– 1 mA cm^{-2}; **– 3 mA cm^{-2}.

The pH charge profile is, on the contrary, nonlinear in nature and shows that the greatest charge in acidity takes place in the first quarter of the diffusion layer as in Figure 3b.

Thus, for the first time we calculated the concentration of complex particles on the cathode surface and in the near-electrode layer in a solution containing the unprotonated complex $[SnCit]^{2-}$. The calculation shows an increase in the pH of the cathode layer in the electrolysis process by more than 2.5 units, which indicates that the composition of the particles in the solution volume and on the surface is significantly different, especially for acid electrolytes as described in the literature. In such solutions, the discharge of hydrogen ions, protonated citric acid ions, and protonated forms of tin citrate with evolution of hydrogen leads to strong alkalization

and therefore to deprotonation of the tin electroactive complex, and when considering the mechanism of electroreduction of a metal, this fact must be taken into account. That is, as obtained experimentally for pH 4.6–5.6, voltammetric dependencies refer to unprotonated tin citrate.[7] Calculation of the distribution of complex particles in the diffusion layer and on the surface makes it possible to determine the composition of the electroactive particle discharged at the electrode and shows the need to include the deprotonation stage in the discharge mechanism as a precursor chemical stage. Therefore, we consider it necessary to clarify the discharge mechanism for $[HSnCit]^{3-}$ indicated in the literature. The study of the kinetics of the cathodic reaction in a solution containing only $[SnCit]^{2-}$ avoids the parallel discharge of other tin-containing particles, precludes the possibility of the preceding chemical stage, and ensures that certain kinetic parameters belong to the category of this complex.

2.3. Study of the kinetics of tin electroreduction

The electroreduction of a tin(II) citrate complex was studied by stationary and nonstationary voltammetry. Since two parallel processes occur at the cathode, namely the formation of a metal and the evolution of H_2, in order to determine the kinetic parameters and mechanism of tin electroreduction from citrate complexes it is necessary to single out the partial dependence of each process. For this the current efficiency of tin deposited and hydrogen evolved on the cathode from a citrate electrolyte at pH 8.0 and 25 °C has been determined. The cathode current efficiency (CCE) was calculated according to Faraday's law from the cathode weight gain:

$$CCE(Sn) = \frac{m(g)}{k_{Sn}(g/A \cdot h) \cdot I(A) \cdot \tau(h)}. \tag{18}$$

The rest of the current is due to hydrogen reduction. The particular polarization curves of the parallel processes of metal and hydrogen evolution were calculated from the dependence at each particular point:

$$j_i = j_{\sum} \cdot fCCE_i(j_{\sum}), \tag{19}$$

where j_i is the partial current of tin or hydrogen; fCCE (j_{Σ}) is the current output function of the polarizing current density.

The dependence of the current efficiency of tin on polarizing current density is shown in Figure 4a. As seen from Figure 4a, the current efficiency of tin decreases only slightly with increasing current density, i.e. when the current density increases to 5.0 mA cm^{-2}, the current efficiency of the desired metal decreases by only 6%. The current efficiency of hydrogen increases in proportion to this. Using this information, the experimental stationary polarization curve was divided into partial curves as shown in Figure 4b.

The experimental polarization curve exhibits an initial deceleration portion and then a rise to a limiting current plateau, the vague shape of which and the further rise of the curve are both due to the hydrogen evolution process.

The partial polarization curve of tin reduction coincides at the initial stage with the overall experimental curve and then rises to a well-defined limiting current plateau. The partial curve for hydrogen rises smoothly on potential shifts with more negative values by the exponential law in accordance with the equation of delayed discharge.

Figure 5 shows the morphology of the surface of electrolytic tin deposited at a current density of 7.5 mA cm^{-2} and a temperature of 20 °C, i.e. in the region of diffusion control of the process.

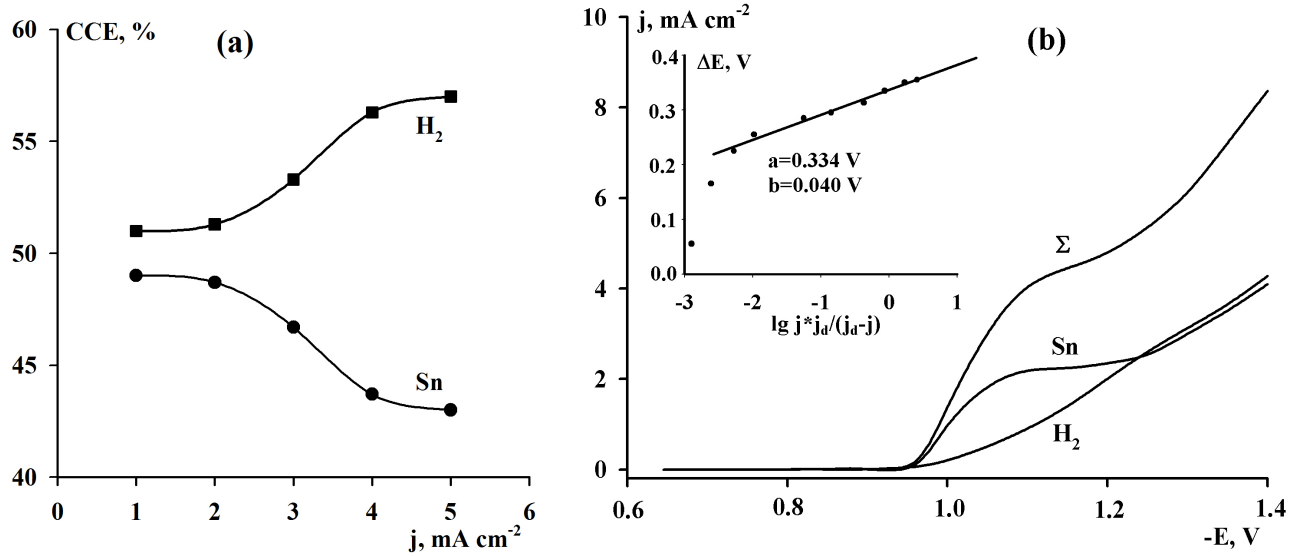

Figure 4. Dependence of the CCE of tin and hydrogen on polarizing current density (a); division of the overall voltammetric curve into partial curves and Tafel plot (b).

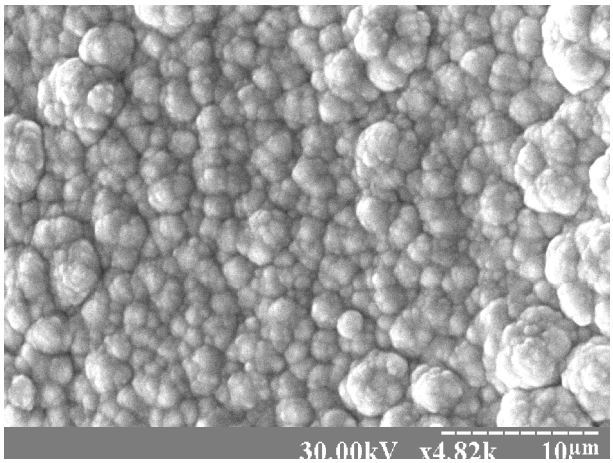

Figure 5. SEM image of the surface of the tin coating.

It can be seen that under such an electrolysis regime that a coating of spherulitic morphology with a developed surface is formed, which is a prerequisite for the effective operation of tin coatings as the anodes of Li-ion batteries.

To determine the kinetic parameters of the process of tin deposition from the citrate electrolyte, the partial polarization curve for tin was represented with allowance for diffusion in the $\Delta E - lg(j \times j_d/(j_d - j))$ coordinates. In that case, the slope was 40 mV, and the exchange current density was $j_0 = 3.35 \times 10^{-9}$ mA cm^{-2}, where j_d is the density of the limiting diffusion current.

Analogous calculations for the anodic branch of the polarization curve give a Tafel slope value of 120 mV. Based on all said above, it can be concluded that the electroreduction of tin(II) citrate complex involves a slow second-electron transfer step.[14]

To correctly describe the electroreduction mechanism of the complexes, information on the order of

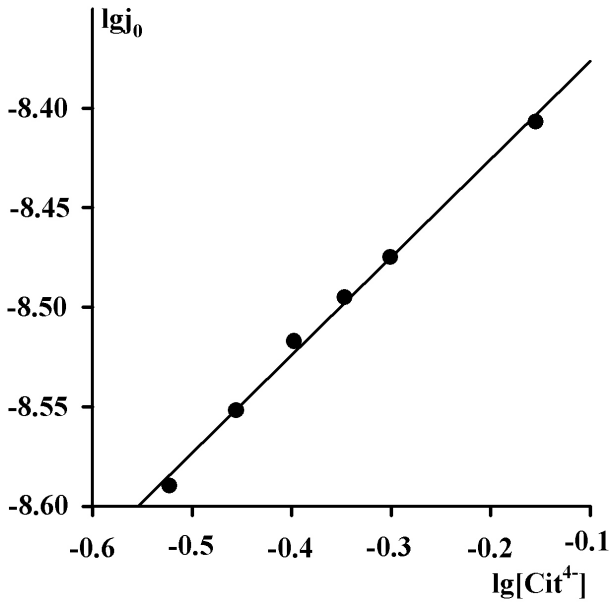

Figure 6. Dependence of exchange current on the citrate concentration in the electrolyte.

reactions is required. Figure 6 shows a plot of exchange currents of a cathode reaction against the citrate concentration in the electrolyte. As seen from the figure, this plot is rectilinear in nature, and its slope is 0.5.

The overall electrode reaction in this case is of the following from:

$$[SnCit]^{2-} + 2e \Leftrightarrow Sn + Cit^{4-}. \tag{20}$$

At the values of the stoichiometric coefficient found from the overall electrode reaction ($\nu_{SnCit} = 1$, $\nu_{Cit} = -1$, $\nu_{Sn} = -1$, $n = 2$, $z = 2$), and from the data presented in Figure 6, in accordance with Eq. (21), described in a previous work,[15] we obtain the order of electrochemical reaction for citrate ions, $z_{Cit} = 0$.

$$z_{Cit} = \frac{\partial \lg j_0}{\partial \lg C} + (1-\alpha)\,\nu_k \cdot \frac{z}{n} \tag{21}$$

The results of chronovoltammetric studies are presented in Figure 7. The plot of peak current against $\sqrt{v}$ (Figure 7a) is a straight line passing through the origin of coordinates, which makes it possible, in accordance with Eq. (22) in a previous work,[16] to calculate the diffusion coefficient of the ions being discharged.

$$j_p = 3 \cdot 10^5 n\,(\alpha n_\alpha)^{1/2}\, AD^{1/2}\nu^{1/2}C^0 \tag{22}$$

Thus, the experimentally determined diffusion coefficient of electroactive $[\mathrm{SnCit}]^{2-}$ ions was $\mathrm{D} = 1.0 \times 10^{-6}$ $\mathrm{cm}^2\ \mathrm{S}^{-1}$.

The potential shift yielding more negative values upon increase in scan rate and the linear dependence of peak potential on the logarithm of potential scan rate indicate that an irreversible process occurs at the cathode (Figure 7b).

Based on the values of the kinetic parameters and the nature of the rate-determining step, a tin(II) citrate electroreduction mechanism can be proposed:

$$[SnCit]^{2-} + e \Leftrightarrow [SnCit]^{3-}, \tag{23}$$

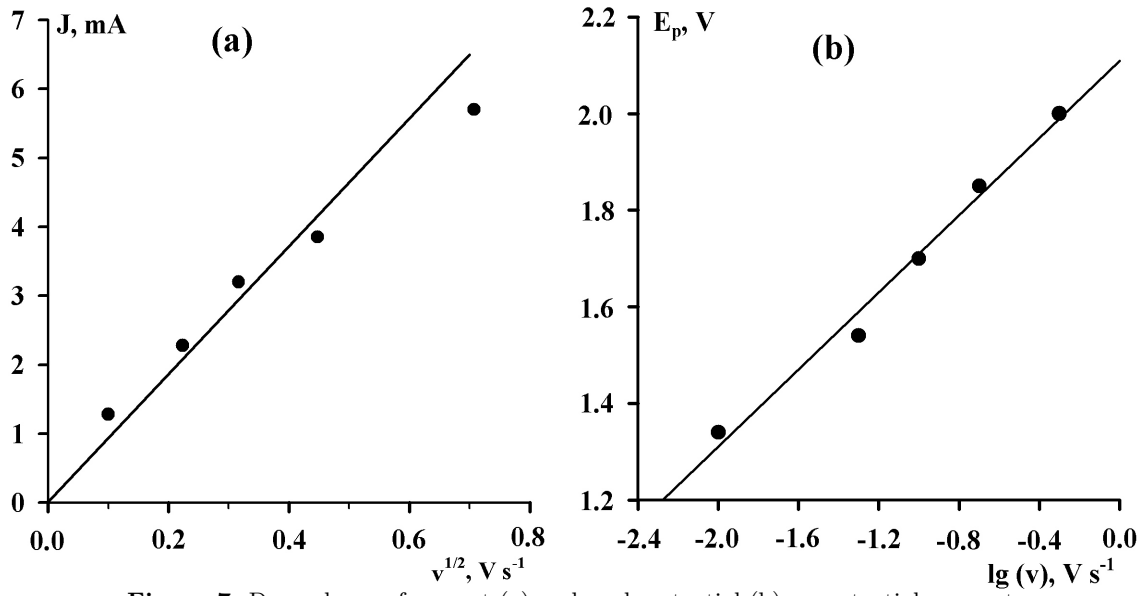

Figure 7. Dependence of current (a) and peak potential (b) on potential scan rate.

$$[SnCit]^{3-} + e \rightarrow [SnCit]^{4-}, \tag{24}$$

$$[SnCit]^{4-} \rightarrow Sn^0 + [Cit]_s^{4-}, \tag{25}$$

where the $[\mathrm{SnCit}]^{2-}$ species is actually electroactive. In a previous work[7] it was suggested that $[\mathrm{SnCit}]^{2-}$ can be an electroactive complex along with $[\mathrm{HSnCit}]^{-}$, but on the basis of our calculations it was proved that the unprotonated citrate complex is an electroactive particle that discharges to form a metal.

The dependences calculated in our work allow us to determine the range of the operating current densities for obtaining dense fine-crystalline coatings (the kinetic control region is up to 4 mA cm^{-2} on the polarization curve) and for obtaining larger crystalline coatings having pores and surface defects (the diffusion control region is more than 6 mA cm^{-2} on the polarization curve), ideally suited for the lithium intercalation process when anodes work in Li-ion batteries.

2.4. Conclusions

The kinetic parameters of the cathodic process and the reaction order for ligand ions have been determined by stationary voltammetry and chronovoltammetry. Based on experimental data, a mechanism of electroreduction of the electroactive complex $[\mathrm{SnCit}]^{2-}$, which involves a slow second-electron transfer step, has been proposed.

It has been shown that the current efficiency of tin in the proposed citrate electrolyte is 52%–57%. The diffusion coefficient of the ion being discharged has been determined to be $\mathrm{D} = 1.0 \times 10^{-6}$ cm^2 s^{-1}.

The working current densities are determined, allowing for the deposition of functional tin coatings: fine-crystalline up to 4 mA cm^{-2} for protection from corrosion and decorative finish and large-crystal above 6 mA cm^{-2} for anode coatings of Li-ion batteries.

It is shown that an electrolyte containing an excess of a ligand makes it possible to completely bind metal ions to a complex, and the stronger the complex, such as $[\mathrm{SnCit}]^{2-}$, the greater the initial deceleration on the current-voltage curve and the more negative the potential for the beginning of the release of the metal. This

makes it possible to bring together the potentials of electroreduction with, for example, copper to form an electrolytic alloy.

3. Experimental

The research was carried out in solutions containing 0.1 mol L^{-1} $SnSO_4 \cdot 5H_2O$ and 0.5 mol L^{-1} Na_3Cit, while 0.5 mol L^{-1} Na_2SO_4 was used as the supporting electrolyte. Analytically pure salts were used to prepare solutions. A platinum plate was used as the working electrode, whose surface was coated before each experiment with a 10-µm copper layer from an acid sulfate electrolyte and then with a tin layer from the working electrolyte in order to eliminate crystallization overpotential. The auxiliary electrode was a platinum wire, and the reference electrode was a saturated silver-silver chloride electrode. All experiments were performed in a thermostated cell at a temperature of 20 °C, which was controlled with an accuracy of ±0.1 °C. To take j-E curves, a PI-50-1.1 potentiostat with PR-8 programmer and LKD4-003 X-Y recorder was used. The stationary voltammetric curves were recorded under potentiodynamic conditions at a potential scan rate of 2 mV s^{-1}. The chronovoltammetric investigations were carried out in a potential scan rate range of 5–100 mV s^{-1}.

References

1. Goriparti, S.; Miele, E.; De Angelis, F.; Di Fabrizio E.; Zaccaria R. P.; Capiglia C. *Journal of Power Sources* **2014**, *257*, 421-443.
2. Bin, W.; Bin, L.; Xianglong, .i; Linjie, Z. *Materials Today* **2012**, *15*, 544-552.
3. Kublanovsky, V. S.; Nikitenko, V. N.; Globa, N. I. *Russian Journal of Applied Chemistry* **2015**, *88*, 407-412.
4. Yapontseva, Yu. S.; Bersirova, O. L.; Kublanovsky, V. S. *Metallofizika i Noveishie Tekhnologii* **2006**, *28*, 91-96.
5. Survila, A.; Mockus, Z.; Jusienas, R.; Jasulaitiene, V. *J. Appl. Electrochem.* **2001**, *31*, 1109-1116.
6. He, A.; Liu, Q.; Ivey, D. G. *J. Mater. Electron.* **2008**, *19*, 553-562.
7. Survila, A.; ockus, Z.; Kanapeckaite, S. *Electrochim. Acta* **2000**, *46*, 571-577.
8. Han, C.; Liu, Q.; Ivey, D. G. *Electrochim. Acta* **2008**, *53*, 8332-8340.
9. Bersirova, O.; Kublanovsky, V.; Cesiulis, H. *ECS Trans.* **2012**, *50*, 155-163.
10. Sillen, L. G.; Martel, A. E. *Stability Constants of Metal-Ion Complexes/Special Publication;* Chemical Society: London, UK, 1971.
11. Zoski, C. G. *Handbook of Electrochemistry*; Elsevier: Amsterdam, the Netherlands, 2007.
12. Survila, A. *Electrochemistry of Metal Complexes: Application from Electroplating to Oxide Layer Formation*; Wiley-VCH: Weinheim, Germany, 2015.
13. Ibl, N.; Barrada, Y.; Trumpler, G. *Helv. Chim. Acta* **1954**, *37*, 583.
14. Damaskin, B. B.; Petrii, O. A.; Tsirlina, G. A. *Electrochemistry*; Chimiya, Koloss: Moscow, Russia, 2006.
15. Vetter, K. J. *Electrochemical Kinetics: Theoretical Aspects*; Academic Press: New York, NY, USA, 1967.
16. Danilov, F. I.; Protsenko, V. S. *Linear and Cyclic Voltammetry V. 1*; Lira: Kyiv, Ukraine, 2016.